

Article

The Treatment of Natural Calcium Materials Using the Supercritical Antisolvent Method for CO₂ Capture Applications

Luís C. S. Nobre ¹, Paula Teixeira ^{2,*}, Carla I. C. Pinheiro ², António M. F. Palavra ², Mário J. F. Calvete ³, Carlos A. Nieto de Castro ¹ and Beatriz P. Nobre ^{2,*}

¹ Centro de Química Estrutural, Institute of Molecular Sciences, Departamento de Química e Bioquímica, Faculdade de Ciências, Universidade de Lisboa, Campo Grande, 1749-016 Lisboa, Portugal; luiscs.nobre@gmail.com (L.C.S.N.); cacastro@ciencias.ulisboa.pt (C.A.N.d.C.)

² Centro de Química Estrutural, Institute of Molecular Sciences, Departamento de Engenharia Química, Instituto Superior Técnico, Universidade de Lisboa, Av. Rovisco Pais, 1049-001 Lisboa, Portugal; carla.pinheiro@tecnico.ulisboa.pt (C.I.C.P.); antonio.palavra@tecnico.ulisboa.pt (A.M.F.P.)

³ Centro de Química de Coimbra, Institute of Molecular Sciences, Departamento de Química, Universidade de Coimbra, 3004-535 Coimbra, Portugal; mcalvete@qui.uc.pt

* Correspondence: paula.teixeira@tecnico.ulisboa.pt (P.T.); beatriz.nobre@tecnico.ulisboa.pt (B.P.N.)

Abstract: The potential of the supercritical antisolvent micronization (SAS) technique was evaluated for the production of CaO-based particles with a size and a physical structure that could enable high performance for CO₂ capture through the calcium looping process. Two sources of calcium derivative compounds were tested, waste marble powder (WMP) and dolomite. The SAS micronization of the derivate calcium acetate was carried out at 60 °C, 200 bar, a 0.5 mL min⁻¹ flow rate of liquid solution, and 20 mg mL⁻¹ concentration of solute, producing, with a yield of more than 70%, needle-like particles. Moreover, since dolomite presents with a mixture of calcium and magnesium carbonates, the influence of the magnesium fraction in the SAS micronization was also assessed. The micronized mixtures with lower magnesium content (higher calcium fraction) presented needle-like particles similar to WMP. On the other hand, for the higher magnesium fractions, the micronized material was similar to magnesium acetate micronization, presenting sphere-like particles. The use of the micronized material in the Ca-looping processes, considering 10 carbonation-calcination cycles under mild and realistic conditions, showed that under mild conditions, the micronized WMP improved CaO conversion. After 10 cycles the micronization, WMP presented a conversion 1.8 times greater than the unprocessed material. The micronized dolomite, under both mild and real conditions, maintained more stable conversion after 10 cycles.

Keywords: supercritical antisolvent method; marble; dolomite; CO₂ capture; micronization



Citation: Nobre, L.C.S.; Teixeira, P.; Pinheiro, C.I.C.; Palavra, A.M.F.; Calvete, M.J.F.; Nieto de Castro, C.A.; Nobre, B.P. The Treatment of Natural Calcium Materials Using the Supercritical Antisolvent Method for CO₂ Capture Applications. *Processes* **2024**, *12*, 425. <https://doi.org/10.3390/pr12030425>

Academic Editors: Federica Raganati and Paola Ammendola

Received: 21 November 2023

Revised: 13 February 2024

Accepted: 15 February 2024

Published: 20 February 2024



Copyright: © 2024 by the authors. Licensee MDPI, Basel, Switzerland. This article is an open access article distributed under the terms and conditions of the Creative Commons Attribution (CC BY) license (<https://creativecommons.org/licenses/by/4.0/>).

1. Introduction

Sustainability and sustainable development are the goals that society seeks to achieve. The United Nations Organization (UNO) has been promoting these goals since the publication of the Brundtland Report [1] in 1987. Now, they have established a Sustainable Agenda until the year 2030 [2] and therein proposed 17 objectives, including some concerning the energetic and resource areas. On the other hand, the European Union (EU) research and innovation framework program, Horizon Europe (HE), aims to pursue breakthrough solutions for the major challenges that economies and societies face today in environmental, energy, digital, and geopolitical areas. Chemistry has made important contributions to meeting the goals of this Agenda and to the previous goals of the UNO. A field very much explored, and where considerable work can still be carried out, is the valorization of natural resources and the reuse of waste materials. Waste materials, for instance, from heavy or construction industries, are a major environmental problem, presenting a threat to the environment [3–6]. However, as previously stated, industrial waste can be an interesting

source of valuable compounds, such as manganese obtained from silico-manganese waste slag [7], magnesium from industrial effluents [8], or rare earth metals from secondary sources, such as coal ash, red mud, or phosphogypsum [9]. Another important example is the reuse of sources of calcium. There is great availability of this element in nature, such as minerals like limestone and other minerals containing calcium in carbonated form, or in shells of eggs or mussels, foods widely appreciated and with industrialized production. There are several applications for calcium in different forms. The most used is the oxide form, which has many applications, for instance, as a catalyst for the transesterification reaction of fatty acids to produce biodiesel [10]. In the form of acetate salt, it can be used as a food and beverage additive or as an active pharmaceutical ingredient to treat kidney problems [11].

These calcium materials' natural resources can be used, on a large scale, to capture CO₂ and can also be used as an agent to produce energy combined with renewable energies. The process to capture CO₂, also known as calcium looping (CaL), uses a CaO-based sorbent reacting via the reversible reaction of the calcination of CaCO₃ [12–16]. Another application of this calcium looping system is in concentrated solar power (CSP) systems [17,18]. In these systems, the CaCO₃ is decomposed into CaO and CO₂ at the calcination stage when absorbing solar energy, and when the sunlight is weak at night, an exothermic reaction between CaO and CO₂ takes place to retrieve the thermal energy and reform CaCO₃. The key barrier to CaL is the sintering with cycling. Some ways to overcome this issue include the chemical pretreatment of materials, the synthesis of nano-CaO, and the use of CaO with a dopant. One that is widely used is Mg [19,20] due to the high Tammann temperature of MgO (1276 °C) [20]. In nature, it is possible to find it combined with calcium in dolomite Ca_(1-x)Mg_x(CO₃)₂, a mineral that contains calcium and magnesium carbonates in different proportions. The use of these materials in the referred applications is in raw form, with them undergoing grind processes to reduce their size. But this generates very heterogeneous materials in terms of morphology, size, and the particle size distribution of the produced particles and even some wastage.

To overcome the limitations of the physical processes, several methods to prepare micro and nanoparticle metal oxides have been developed. The so-called conventional methods include processes like aqueous phase precipitation, sol-gel chemistry, and gas-phase polymerization. The use of supercritical techniques such as supercritical antisolvent precipitation (SAS), which is included in the classification of non-conventional techniques [21], can also be a suitable alternative for the preparation of nanoparticles of metal oxides. The SAS process involves, most of the time, CO₂ as the supercritical fluid (scCO₂). The reason it is a better environmental option is because CO₂ can be obtained with high purity from natural sources (apart from the ones that make it necessary to capture it from the atmosphere and industrial processes). It also has non-inflammable properties, low toxicity, and an easily achieved critical point. To successfully carry out this process, the supercritical antisolvent needs to be completely miscible with the liquid solvent used during the process, whereas the solute to be micronized has to be insoluble in the mixture solvent/scCO₂. During this process, the diffusion of scCO₂ in the liquid solvent is very fast, since the diffusivity of scCO₂ is about two orders of magnitude higher than that of conventional liquids, which produces the supersaturation of the solute immediately before its precipitation, leading to the production of nanoparticles. Depending on the process parameters that influence the supersaturation and the nucleation rate, the particle size, particle morphology, and particle size distribution can vary over a wide range and can be tuned. The SAS process has already been explored to prepare metal oxide precursors, mainly catalysts [22–24] and superconductors [25,26], but to our knowledge, its use to produce CaO-based sorbents for CO₂ capture is not described in the literature.

In this study, two natural calcium-based materials, a waste marble powder and a dolomite, were treated using the SAS technique. The performance of both materials, before and after treatment, was evaluated along with the CaL process performed under mild (800 °C) and realistic (930 °C) calcination conditions. The effect of MgO content on the

sorbent's CO₂ capture performance was also evaluated through the preparation of synthetic mixtures using commercial calcium and magnesium acetates as precursors.

2. Materials and Methods

2.1. Materials

Waste marble powder (WMP) and dolomite powder were obtained from the Portuguese cutting and polishing marble industry and a Turkey quarry, respectively. Both materials were used as supplied. DMSO (CAS numbers 67-68-5) was provided by Merck with a purity of 99.9%, and glacial acetic acid (64-19-7) was procured from Chem-Lab. Calcium acetate and magnesium acetate, p.a. grade from Carlo Erba, were used as precursors of synthetic CaO/MgO mixtures. Both chemicals were used as supplied.

2.2. Preparation of the Calcium Materials

The CaCO₃ and MgCO₃, present in the marble and dolomite, were transformed into calcium acetate and magnesium acetate, respectively, using aqueous acetic acid (30% in mass) following the procedure described in reference [27]. The reaction was considered complete when all of the carbonates disappeared and no more CO₂ was released. Afterward, the remaining inorganic material (e.g., impurities from the natural material) was filtrated, and the calcium and/or magnesium acetate solution was recovered, with the solvent being evaporated through the use of a vacuum rotary evaporator. Finally, the organic solution to be used in the SAS process, which contained the compounds to be micronized, was prepared by solubilizing the calcium acetate and/or magnesium acetate in a solvent mixture of DMSO and acetic acid (50/50 *v/v*).

Moreover, for comparative reasons and to assess the effect of the MgO mass fraction (wt., %) in the sorbent's CO₂ capture performance and stability, mixtures with 10%, 20%, 30%, and 40% of calcium and magnesium were prepared using the corresponding commercial acetates (corresponding to 92/8; 83/17; 75/25; and 65/35 of CaO/MgO). These mixtures were also solubilized in the solvent mixture (DMSO/acetic acid 50/50 *v/v*) to be used in the SAS process.

2.3. Characterization of the Materials

The chemical composition of the WMP and dolomite was determined at LAIST (Laboratory of Analysis of Instituto Superior Técnico). The oxide content of calcium, magnesium, aluminum, silicon, potassium, and iron was determined via an inductively coupled plasma optical emission spectrometer, and carbon was quantified using an internal method.

The textural properties of fresh natural materials, after micronization, and commercial calcium acetate were determined through N₂ sorption at −196 °C on a Micromeritics ASAP 2010 apparatus. To remove water, the samples were outgassed under vacuum at 90 °C for 1 h and then at 120 °C for 5 h. The BET equation was applied to estimate the specific surface area (S_{BET}), the total pore volume (V_{p}) was calculated from the adsorbed volume of nitrogen for a relative pressure (p/p_0) of 0.97, and the pore size distribution (PSD) was obtained by using the BJH model (desorption branch).

The morphology and particle size were analyzed by scanning electron microscopy (SEM), using an Analytical FEG-SEM JEOL 7001 F with Oxford light elements, an EDS detector, and an EBSD detector.

The mineralogical phases of the treated sorbents, before and after micronization, were investigated using X-ray powder diffraction (XRD) in a Bruker D8 Advance diffractometer set up with a 1D detector (SSD 160), a Cu K α ($\lambda = 0.15406$ nm), and a Ni filter. Each sample was scanned within the 2θ range of 5–80°, with a step size of 0.03° and a step time of 0.5 s. The PDF database was used to identify the crystalline phases.

2.4. Supercritical Antisolvent Precipitation

The SAS apparatus used to perform the micronization experiments was previously described in detail [27,28] and is presented in Figure 1. It consists of a co-current precipitator,

fed separately to the top of the chamber by the supercritical fluid and the liquid solution, continuously discharged from the bottom. Two HPLC pumps (Gilson 306) were used to deliver the supercritical CO₂ and the liquid solution. To avoid cavitation due to the pumping of a compressible fluid, the CO₂ and the head of the pump were previously cooled in an ice bath. The two streams were heated in a thermostatic bath before entering the precipitation chamber with a cylindrical vessel of 300 mL. The organic solvent (solvent mixture of DMSO and acetic acid 50/50 *v/v*) containing the solute to be precipitated was injected into the precipitator through a stainless-steel nozzle with a 125 μm internal diameter and a 1 cm length, located on the top of the vessel. The pressure and temperature inside the precipitator were monitored with a transducer P X 435 (Omega Engineering Inc., Norwalk, CT, USA), and thermocouple type J (Omega Engineering Inc.) with an uncertainty of ±0.2 bar and ±0.3 °C, respectively. A stainless-steel frit was used to collect the micronized compound at the bottom of the precipitator, where the mixture of supercritical CO₂ and organic solvent can pass through. The solvent mixture's flow rate is controlled by a micrometric valve and, after the solvent mixture is separated, the liquid solvent is recovered, with the separation pressure being regulated by a back-pressure valve. Afterward, decompressed CO₂ passes through a rotameter and a wet test meter to measure the flow rate and the quantity of CO₂ used, respectively.

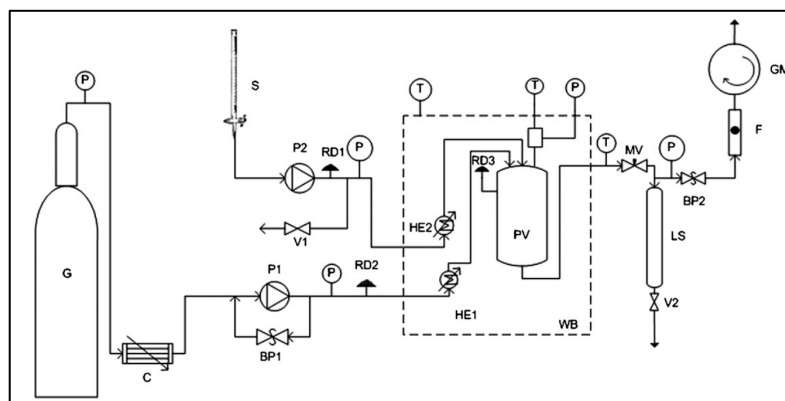


Figure 1. Schematic diagram of the SAS apparatus. BP1 and BP2—back pressure regulators; C—CO₂ cooler; F—calibrated flow meter; G—CO₂ cylinder; GM—dry test meter; HE1 and HE2—heat exchangers; LS—liquid solvent recover vessel; MV—micrometering valve, P—pressure transducer, T—temperature sensor.

The experimental conditions to precipitate the metallic acetates produced from marble and dolomite, and from the CaO/MgO commercial mixtures, were chosen according to the optimization performed in a previous study using eggshells [27]. The optimal experimental conditions to carry out the SAS micronization of calcium acetate dissolved in a solvent mixture of DMSO and acetic acid (50/50 *v/v*) were: a temperature of 60 °C; pressure of 200 bar; a solute concentration of 20 mgmL⁻¹; and an organic solution flow rate of 0.5 mLmin⁻¹.

2.5. Cyclic Carbonation–Calcination Tests in a Thermogravimetric Analyzer

The multicycle CO₂ capture behavior of the fresh and SAS micronized sorbents was assessed using a thermogravimetric analyzer (TGA) system TG-DSC Setsys Evo 16. In our previous study [20], it was found that the most remarkable deactivation processes occurred for cycles 1 to 10, while the results were considerably similar in the 10th to 20th cycle range. Consequently, tests with 10 carbonation–calcination cycles were carried out in this work. For each experiment, ca. 5 mg of sample was used and a CO₂, air, or CO₂/air flow of 40 mLmin⁻¹ was used during the carbonation–calcination cycles. First, the sorbents were pre-activated at 800 °C or 930 °C under air or CO₂ atmosphere, respectively, to guarantee that before the first carbonation process, all of the sorbent was present as an oxide. Then, carbonation was carried out using a gas mixture with a CO₂ concentration

of 25% to mimic the real flue gas CO₂ concentration balanced in the air (700 °C, 60 min), followed by calcination under an air or CO₂ atmosphere (800 or 930 °C, 10 min). The lower pre-activation/calcination temperature, i.e., 800 °C, was used only for comparative reasons. Calcination at 930 °C, under a pure CO₂ atmosphere, is more realistic for the industrial applications foreseen in CO₂ storage or utilization. The mass variation during the carbonation and calcination of each cycle came from the CO₂ that is captured and released along the cycles, which allowed for the calculation of the moles of CO₂ that are captured in each carbonation step ($n_{\text{CO}_2, \text{carb}}$). Then, the CO₂ conversion of each sorbent was calculated by using the ratio of the number of CO₂ moles captured during each cycle's carbonation step, and the theoretical number of moles that can be captured in relation to the CaO content in the sample is described by Equation (1):

$$\text{CaO}_{\text{conversion}} = \frac{n_{\text{CO}_2, \text{carb}} \times M_{\text{CaO}}}{m_{\text{sorbent}} \times w_{\text{CaO}}} \times 100(\%) \quad (1)$$

where M_{CaO} is the molar mass of CaO, m_{sorbent} is the initial mass of the sorbent, and w_{CaO} is the percentage of CaO in the sorbent. For the natural materials, the CaO content was estimated through the chemical analysis of the fresh materials. A blank experiment was conducted to correct apparatus buoyancy effects like atmosphere density changes with temperature.

The carbonation rate ($\partial X_n / \partial t$), where $X_n = m_{\text{CO}_2 \text{ captured}} / m_{\text{CaO}}$ and t is the time, was estimated for the 1st and 10th cycle carried out in the TGA (the data acquisition interval was 2 s).

3. Results

3.1. Properties of Natural Calcium Materials and Precipitated Products

The oxide content of the fresh WMP and dolomite sorbent samples, dried at 120 °C, is presented in Table 1.

Table 1. Oxide content of fresh WMP and dolomite materials dried at 120 °C.

Oxide Content wt. (%)	SiO ₂	CaO	MgO	Al ₂ O ₃	Fe ₂ O ₃	K ₂ O	CO ₂
WMP	1.50	52.2	0.45	0.23	0.11	0.12	44.0
Dolomite	0.09	34.8	17.1	0.02	0.01	n.d.	46.2

The fresh natural WMP and dolomite samples were analyzed using SEM analysis (Figure 2). The WMP contains particles with a larger size than the dolomite sample, and most of them show a cubic appearance. On the other hand, the dolomite sample is composed of a mixture of larger- and smaller-sized particles that, based on the energy dispersive X-ray spectroscopy (EDS) analysis, correspond to CaCO₃ and MgCO₃ particles, respectively.

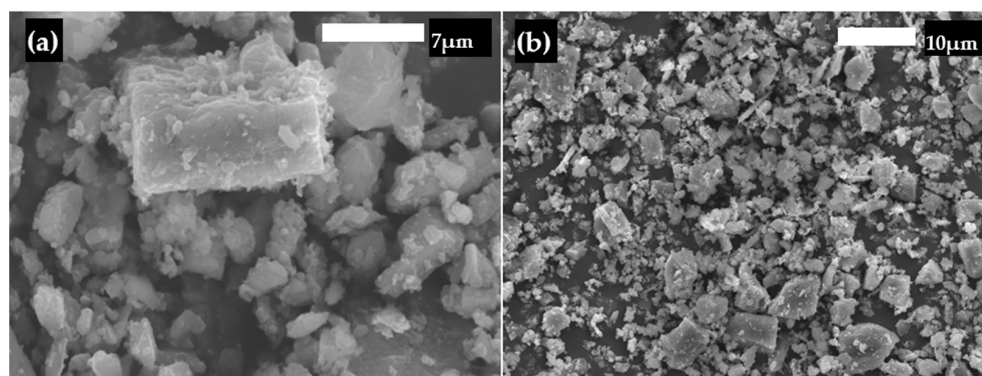


Figure 2. SEM images of fresh (a) WMP and (b) dolomite.

After the SAS process, the morphology of the fresh sample was clearly modified, as is evidenced in Figure 3. For both materials, the particle size reduction was accentuated.

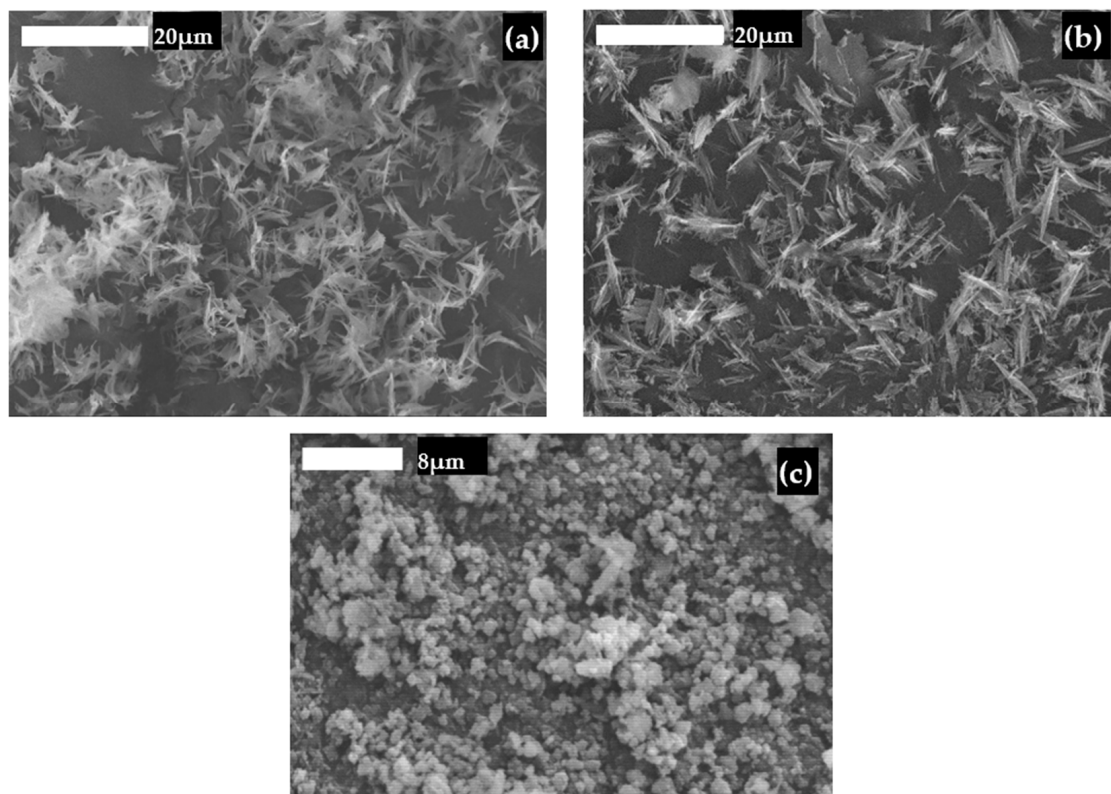


Figure 3. SEM images of SAS micronized compounds obtained with 200 bar of pressure, a 0.5 mL min^{-1} flow rate of liquid solution, and a 20 mgL^{-1} concentration of solute: (a) calcium acetate derived from WMP, (b) calcium acetate produced from eggshells [27], and (c) calcium/magnesium acetates produced from dolomite.

The micronized samples of calcium acetate obtained from WMP were also compared to the calcium acetate processed from eggshells (see the previous work of the authors, reference [27]). Figure 3a,b presents the SEM images of the obtained SAS micronized calcium acetate derived from WMP and eggshells [27], respectively. It can be observed that the source of the material did not affect the final SAS product, and therefore, the micronized calcium acetate derived from waste marble powder presented a similar morphology to that obtained from eggshells, which were needle-like particles (Figure 3a,b). Moreover, the yield of the process was similar for both sources of calcium acetate (>70%). On the other hand, the SAS micronized acetates of Ca and Mg obtained from the dolomite showed a different aspect, presenting considerably smaller particles with sphere-like morphology (Figure 3c).

The effect of the micronization process on the mineralogical structure of calcium-based sorbent obtained from marble samples was assessed. As shown in Figure 4, before micronization, the calcium was present as calcium acetate acetic acid hydrate (PDF 10-0782), but after micronization, only calcium acetate hydrate (PDF 19-0199) was identified, meaning that the SAS process contributes not only to the reduction in calcium acetate particles size but also to sorbent purification.

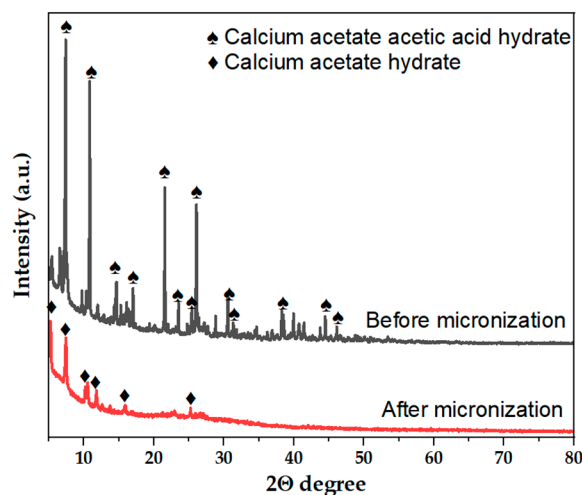


Figure 4. XRD patterns of the marble material after solubilization with acetic acid (30%) before and after the SAS micronization process.

To evaluate how the quantity of magnesium affected SAS micronization and changed the particle morphology, a micronization study with different ratios of calcium–magnesium mixtures was carried out. For this purpose, synthetic mixtures of calcium and magnesium acetates were prepared, using the commercial standards, with amounts of 10%, 20%, 30%, and 40% in the mass percentage of magnesium acetate (corresponding to 92/8; 83/17; 75/25; and 65/35 of CaO/MgO after acetate calcination). The SAS micronization of the obtained mixtures was carried out under the same conditions as the previous micronization of WMP and dolomite. In all of the performed SAS experiments, it was possible to attain yields higher than 80% (m/m). The obtained samples were analyzed using SEM, and the morphology of the samples showed differences, as shown in Figure 5. As can be seen, the micronization of the mixture with only 10% magnesium acetate (Figure 5a) led to particles presenting a morphology very similar to the micronized calcium acetate obtained from WMP, with needle-like particles that were very aggregated but also with the presence, in a considerable minor amount, of other small particles presenting sphere-like morphology. This result follows the trend previously observed for calcium acetate derived from different sources, as well as the calcium–magnesium mixture from dolomite. In fact, for lower magnesium fractions (10–20%), e.g., a higher calcium amount (80–90%), the majority of the particles present a needle-like morphology, which is similar to the SAS micronization of the derived calcium acetate obtained from eggshells or marble waste. On the other hand, with the increase in the magnesium fraction in the mixture, there is an increase in smaller particles with a sphere-like morphology. In fact, the samples prepared with 30% magnesium acetate (Figure 5c) presented a morphology identical to the material obtained from natural dolomite: smaller particles with a sphere-like morphology. Moreover, for the mixture with a 40% magnesium acetate composition (Figure 5d), the material obtained was very homogeneous, presenting small particles with a non-defined shape. These particles present a high degree of aggregation, which can be due to small residues of solvent trapped in the structure of the particles or due to the capture of atmospheric moisture, since these metallic acetates have high hygroscopicity.

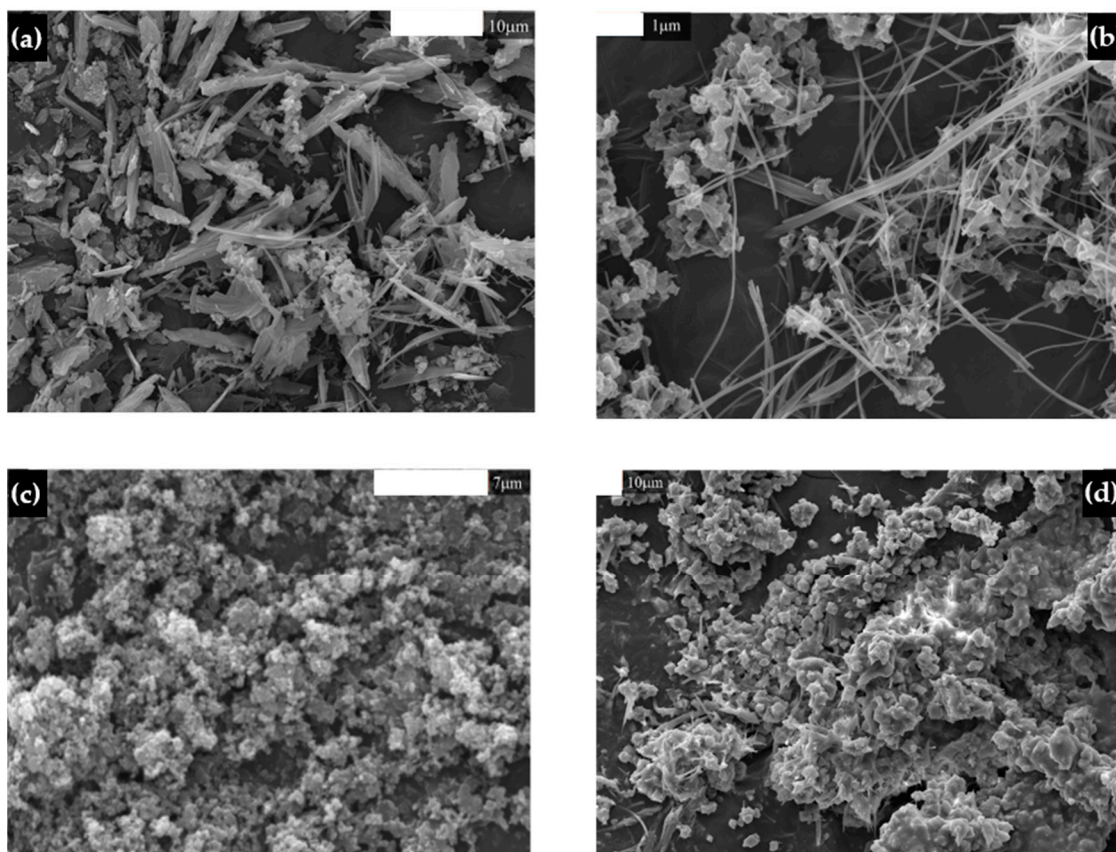


Figure 5. SEM images of Ca/Mg acetates obtained with different ratios of Ca and Mg: (a) 10% Mg; (b) 20% Mg; (c) 30% Mg; (d) 40% Mg.

N_2 sorption studies were carried out for WMP and dolomite samples to evaluate the materials' textural properties, assessing the BET-specific surface area (S_{BET}), total pore volume (V_p), and pore size distribution (PSD) of the SAS micronized materials, as well as the unprocessed sources. For comparison, a commercial calcium acetate sample was also analyzed. The obtained results are presented in Figure 6a,b. From the analysis of the results presented in Figure 6a, it can be seen that, for both materials, i.e., WMP and dolomite, the SAS micronized calcium acetate showed higher S_{BET} and V_p compared to the corresponding unprocessed material (identified above as fresh material). In fact, for the micronized WMP, it was possible to attain a 26-times increase in the specific surface area, whereas, for the micronized dolomite, a more than 30-times increase was observed. On the other hand, the total pore volume of the micronized materials increased more than 23 and 11 times for the WMP and dolomite, respectively. In addition, the comparison of the textural properties of micronized WMP and commercial calcium acetate shows that the S_{BET} and V_p of micronized material increase by 18 and 12 times, respectively. This means that SAS micronization led to a structural arrangement with a considerable increase in porosity, compared to the unprocessed and commercial calcium acetate materials. Since the higher porosity and stability of materials can improve CaO conversion in Ca-Looping, it could be expected that the micronized materials will present higher efficiency in the final process.

Concerning the pore size distribution (results depicted in Figure 6b), there was a strong increase in the pore fraction for the SAS micronized materials compared to the unprocessed sources. The SAS micronized material obtained from WMP maintained its pore size range and presented a considerable increase in the pore fraction for the range of 5–100 nm. Considering that CaO-based sorbents with a pore range from 20–100 nm are regarded as suitable for CO_2 capture [29], the obtained results for micronized WMP

show that the SAS process can improve the structure arrangements towards the use of a CaO-based sorbent for CO₂ capture. Regarding the materials derived from dolomite, it can be seen that the micronization technique led to a material with a strong increase in the pore fraction, though still maintaining the pore size range of the unprocessed material. It can be seen that the increase in the pore volume is considerably strong for pore sizes within the 10–100 μm range, which is also in agreement with the better performance of CaO-based sorbents for CO₂ capture.

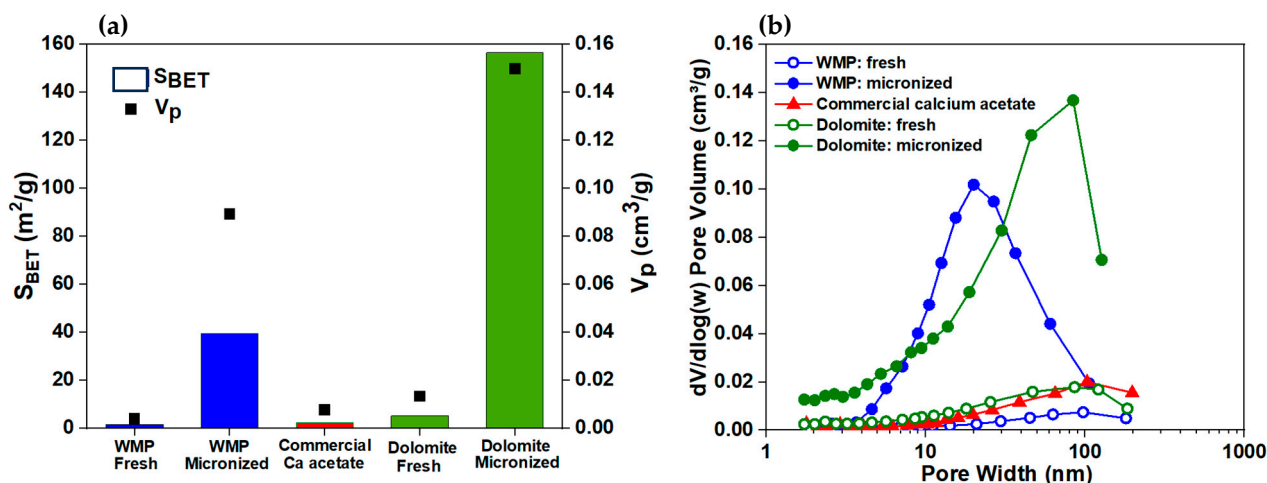


Figure 6. Textural properties of commercial calcium acetate, unprocessed WMP and dolomite and SAS micronized materials: (a) specific surface area (S_{BET} , m^2/g) and total pore volume (V_p , cm^3/g) and (b) BJH pore size distribution (desorption branch).

3.2. Calcium Looping Tests

The micronized materials were submitted to the calcium looping process for post-combustion CO₂ capture. Briefly, the reactivity and stability of the micronized particles were assessed during carbonation–calcination cycles through thermogravimetric analysis (TGA). For practical applications, i.e., CO₂ storage or utilization in conversion processes, CaCO₃-based materials should be calcined in a CO₂-rich atmosphere. However, the thermodynamic equilibrium decomposition of CaCO₃ is a function of CO₂ partial pressure [30,31], meaning that higher temperatures are required if the calcination step is performed under a high CO₂ concentration atmosphere. Indeed, the samples were tested under realist (100% CO₂, 930 °C) and mild (100% air, 800 °C) calcination conditions to evaluate their cyclic CO₂ capture performance. The carbonation conditions were kept constant, with 25% of CO₂ balanced in air, at 700 °C.

Figure 7 presents the results of CaO conversion (%) for 10 carbonation–calcination cycles for the SAS micronized materials, the untreated sources, and commercial calcium acetate tested under mild and realistic calcination conditions.

The sorbent's CaO conversion was determined based on its CaO content because the MgO was already observed to be inert under the experimental conditions tested [20,32]. Under mild conditions, the micronized calcium acetate produced from WMP shows a conversion rate higher than 90% in the first cycle, decreasing only to values of conversion higher than 80% after 10 cycles. Compared with the WMP used without treatment, it is visible that the conversions are much lower than the ones presented for the micronized calcium acetate (~46% vs. 83% after 10 cycles). In comparison with untreated WMP, commercial calcium acetate presents enhanced performance; CaO conversion was ca. 93% and 53% for the 1st and 10th cycle, respectively. However, commercial calcium acetate performs worse than the one produced through the SAS process using WMP as a precursor, evidencing the potential of this technology for the development of CO₂ sorbents using natural source materials.

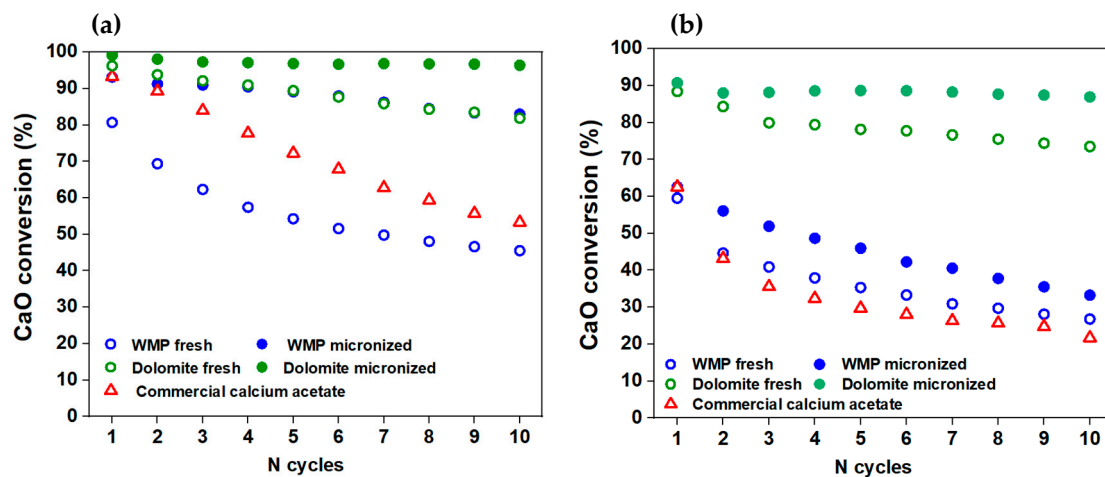


Figure 7. CaO conversion of untreated and micronized WMP or dolomite and commercial calcium acetate during 10 cycles of carbonation at 700 °C and calcination under (a) mild (100% air, 800 °C) or (b) realistic (100% CO₂, 930 °C) calcination conditions.

Regarding the conversion obtained for the micronized calcium acetate and the untreated WMP under realistic conditions, the values during the first cycle are similar; however, the decrease, cycle after cycle, was higher for the untreated sorbent. The deactivation among the 1st and 10th cycles was 55% and 47% (considering the value of the 1st cycle as the reference) for the untreated and micronized WMP, respectively. Opposite to the results observed during mild calcination, the commercial calcium acetate performs worse than the untreated WMP, evidencing its lower sintering resistance to high-temperature calcination. Looking at the results obtained for dolomite treated using the SAS method and the untreated, the maintenance of stability over the 10 cycles, resistance to the sintering effect, and the consequent non-loss of conversion capacity are visible in the untreated sample. These results show that the presence of MgO, which is inert under the used experimental conditions [32], acting only as a CaO particle “spacer”, has a relevant role in the sorbent materials’ stability during the carbonation–calcination cycles. For a better understanding of the SAS process’ effect on the CO₂ capture by CaL, using mild and more realistic calcination conditions (800 °C and 930 °C), the carbonation rate was estimated for the 1st and 10th cycle for the untreated and micronized materials (Figure 8).

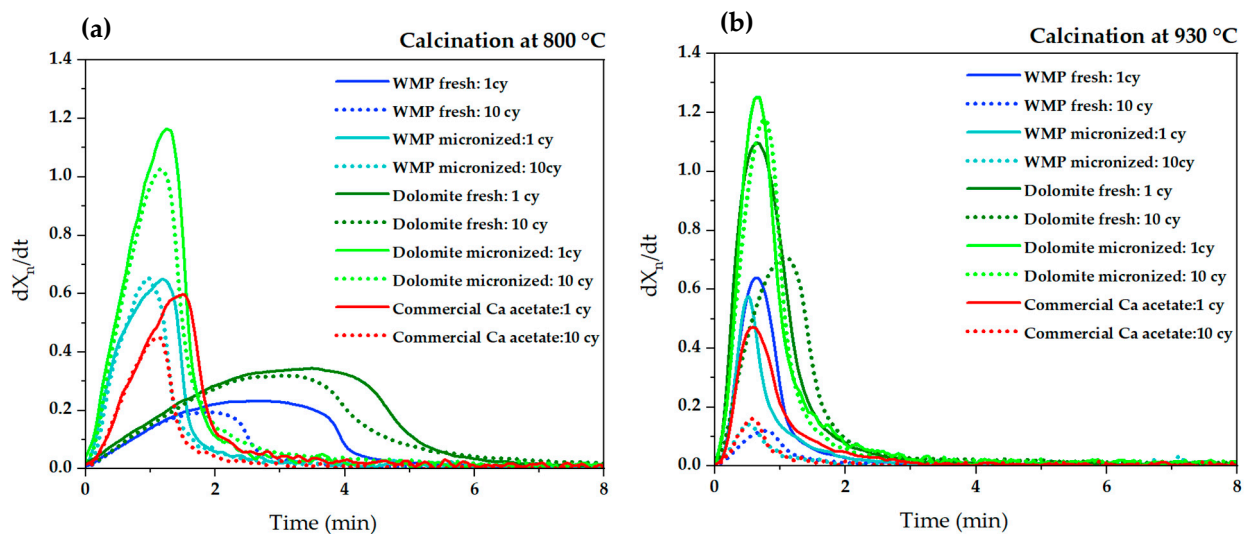


Figure 8. Carbonation rates obtained in a TGA at 700 °C, for the 1st and 10th cycle of the untreated and micronized materials calcined at 800 °C (a) and 930 °C (b).

The carbonation profile of untreated and micronized WMP and dolomite regenerated at 800 °C is very different. For the fresh materials, the carbonation rate is slow; it requires 4–6 min to complete the kinetic stage, while in the case of micronized materials, it is completed after 2 min. This can be justified by the higher specific surface area and total pore volume of the micronized materials (Figure 6a), which facilitates CO₂ diffusion inside the sorbent and favors carbonation. On the other hand, when a higher calcination temperature is used, the carbonation kinetic stage is almost complete after two minutes. Probably, during calcination at a higher temperature, there is a change in the textural properties of sorbents, leading to an increase in their pore size diameter [20], which could favor CO₂ diffusion around the particles, justifying the faster carbonation rate of WMP and dolomite at 930 °C. However, it is expected that CaO sintering also increases, with it being more pronounced for WMP than for dolomite; thus, CaO conversion decreases (Figure 7b). For untreated dolomite, a faster carbonation rate is also observed; however, after 10 cycles, the deactivation is much more accentuated than for the micronized dolomite, evidencing the importance of micronized MgO as a spacer agent. The commercial calcium acetate carbonation rate is usually lower than for the micronized sorbents but faster than the untreated materials.

To evaluate the relevance of the MgO mass fraction on the CaCO₃-based materials' stability during the CaL process, the micronization of four synthetic mixtures of calcium acetate balanced with 10%, 20%, 30%, and 40% magnesium acetate was carried out, which corresponds to 92/8; 83/17; 75/25; and 65/35 CaO/MgO. The micronized samples were tested in the TGA under realistic calcination conditions (Figure 9).

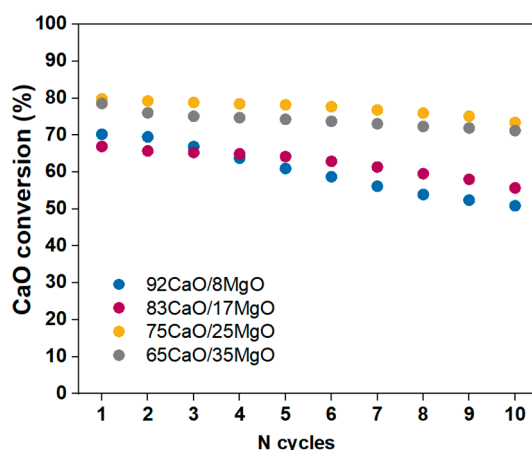


Figure 9. CaO conversion of micronized synthetic mixtures of calcium acetate balanced with 10%, 20%, 30% and 40% magnesium acetate (corresponding to 92/8; 83/17; 75/25; and 65/35 CaO/MgO) during CaL using realistic calcination conditions (100% CO₂, 930 °C).

Figure 9 shows that the sorbents with >25% MgO perform better than those with lower MgO values. The sorbent deactivation was 17–28% for materials with lower MgO content, but it was only 8–9% for materials with more than 25% MgO. The role of MgO in the sorbent's stability has already been studied and described in previous literature works [20,33]. Under CaL experimental conditions, MgO does not capture CO₂ but instead acts as a spacer between CaO particles, avoiding their sintering, which is favored by the high Tammann temperature of MgO (1276 °C). When the MgO content decreases, sorbent deactivation occurs faster because the contact between CaO particles increases, facilitating the coalescence of melted material. Consequently, an increase in CaO crystallites and a decrease in specific surface area occurs, which makes carbonation difficult. Even though MgO contributes to the stability of the sorbent, a compromise between the CaO/MgO ratio must be found in order to be technically feasible and to prevent the building of large carbonation and calcination reactors.

The conversions achieved for the synthetic mixture with 65% CaO and 35% MgO can be directly compared with the micronized dolomite tested under the same conditions

since both contain ca. 65% CaO and 35% MgO after calcination. The results show that the micronized dolomite presents yet lower deactivation (4% vs. 9%) and enhanced CaO conversion after 10 cycles (87% vs. 71%). This agrees with the results achieved for the micronized WMP and commercial calcium acetate (Figure 7), i.e., the micronized sorbents prepared using natural materials perform better than those prepared using synthetic materials as precursors.

4. Conclusions

This work used an environmentally friendly precipitation technique, the supercritical anti-solvent process (SAS), to produce calcium and acetate magnesium particles with improved CaO conversion in Ca-looping for CO₂ capture.

Calcium and magnesium acetate were successfully produced through the SAS process with high yields (>70%), from two different sources: marble and dolomite residues. These results showed that, independent of the starting material, the SAS precipitated material presents similar morphology.

The produced materials were tested for CO₂ capture in a Ca-looping process, for 10 cycles of carbonation–calcination, under realistic and mild calcination conditions and compared with the unprocessed calcium sources (WMP and dolomite). The results showed that the SAS-produced materials had higher CaO conversion in both cases, which can be justified by the increase in the BET surface area and pore volume of the micronized materials, in the 10–100 nm region. Despite the sorbents' deactivation increases when realistic conditions are used, the micronized dolomite always shows higher conversion values compared to the unprocessed materials, as well as the corresponding micronized materials using synthetic calcium or magnesium acetate as precursors. Thus, the SAS process proved to be an efficient technique for the production of high conversion CaO particles to be used in CO₂ capture. This is an innovative concept that joins waste valorization, CO₂ capture, and utilization as feedstock in the SAS process.

Author Contributions: Conceptualization, P.T., L.C.S.N. and B.P.N.; methodology, P.T. and L.C.S.N.; validation, P.T. and L.C.S.N.; investigation, P.T., L.C.S.N. and B.P.N.; writing—original draft preparation P.T., L.C.S.N. and B.P.N.; writing—review and editing, P.T., C.A.N.d.C., C.I.C.P., A.M.F.P., M.J.F.C. and B.P.N.; supervision, P.T. and B.P.N. All authors have read and agreed to the published version of the manuscript.

Funding: This research was funded by FCT through projects UIDB/00100/2020, UIDP/00100/2020, LA/P/0056/2020, and PTDC/EAM-PEC/32342/2017. L.C. Nobre was funded by FCT PD/BD/133309/2017.

Data Availability Statement: All data are reported in the paper.

Acknowledgments: Centro de Química Estrutural is a research unit funded by Fundação para a Ciência e Tecnologia through projects UIDB/00100/2020 (<https://doi.org/10.54499/UIDB/00100/2020>) and UIDP/00100/2020 (<https://doi.org/10.54499/UIDP/00100/2020>). The Institute of Molecular Sciences is an associate laboratory funded by FCT through project LA/P/0056/2020 (<https://doi.org/10.54499/LA/P/0056/2020>). L.C.S.N. acknowledges financial support from the Ph.D. fellowship PD/BD/133309/2017 of the Programa Doutoral FCT “Catalysis and Sustainability” CATSUS (PD/00248/2012). P.T. and B.P.N. acknowledges IST and FCT for the Scientific Employment contract. C.I.C.P. and P.T. acknowledge FCT for the PTDC/EAM-PEC/32342/2017 project funding.

Conflicts of Interest: The authors declare no conflicts of interest.

References

1. Brundtland Commission. *World Commission on Environment and Development*; Elsevier: Amsterdam, The Netherlands, 1987.
2. United Nations. *Transforming Our World: The 2030 Agenda for Sustainable Development*. Available online: <https://sdgs.un.org/2030agenda> (accessed on 22 November 2021).
3. Kumar, A.; Thakur, A.K.; Gaurav, G.K.; Klemeš, J.J.; Sandhwar, V.K.; Pant, K.K.; Kumar, R. A Critical Review on Sustainable Hazardous Waste Management Strategies: A Step towards a Circular Economy. *Environ. Sci. Pollut. Res.* **2023**, *30*, 105030–105055. [[CrossRef](#)]

4. Soliman, N.K.; Moustafa, A.F. Industrial Solid Waste for Heavy Metals Adsorption Features and Challenges; a Review. *J. Mater. Res. Technol.* **2020**, *9*, 10235–10253. [[CrossRef](#)]
5. Melo, J.F.; Junior, J.H.S.; Freire, T.B.d.M.; Rigoti, E.; Pergher, S.B.C.; Martínez-Huitle, C.A.; Castro, P.S. Industrial Waste Reuse: An Alternative Source to Reduced Graphene Oxide for Preparing Electrochemical Sensors. *Electrochim. Acta* **2023**, *454*, 142382. [[CrossRef](#)]
6. Ghisman, V.; Muresan, A.C.; Buruiana, D.L.; Axente, E.R. Waste Slag Benefits for Correction of Soil Acidity. *Sci. Rep.* **2022**, *12*, 16042. [[CrossRef](#)] [[PubMed](#)]
7. Buruiana, D.L.; Obreja, C.D.; Herbei, E.E.; Ghisman, V. Re-Use of Silico-Manganese Slag. *Sustainability* **2021**, *13*, 11771. [[CrossRef](#)]
8. Le, V.G.; Vo, D.V.N.; Tran, H.T.; Duy Dat, N.; Luu, S.D.N.; Rahman, M.M.; Huang, Y.H.; Vu, C.T. Recovery of Magnesium from Industrial Effluent and Its Implication on Carbon Capture and Storage. *ACS Sustain. Chem. Eng.* **2021**, *9*, 6732–6740. [[CrossRef](#)]
9. Gaustad, G.; Williams, E.; Leader, A. Rare Earth Metals from Secondary Sources: Review of Potential Supply from Waste and Byproducts. *Resour. Conserv. Recycl.* **2021**, *167*, 105213. [[CrossRef](#)]
10. Kouzu, M.; Hidaka, J. Transesterification of Vegetable Oil into Biodiesel Catalyzed by CaO: A Review. *Fuel* **2012**, *93*, 1–12. [[CrossRef](#)]
11. Wang, Y.; Xie, G.; Huang, Y.; Zhang, H.; Yang, B.; Mao, Z. Calcium Acetate or Calcium Carbonate for Hyperphosphatemia of Hemodialysis Patients: A Meta-Analysis. *PLoS ONE* **2015**, *10*, 0121376. [[CrossRef](#)] [[PubMed](#)]
12. Erans, M.; Manovic, V.; Anthony, E.J. Calcium Looping Sorbents for CO₂ Capture. *Appl. Energy* **2016**, *180*, 722–742. [[CrossRef](#)]
13. Blamey, J.; Anthony, E.J.; Wang, J.; Fennell, P.S. The Calcium Looping Cycle for Large-Scale CO₂ Capture. *Prog. Energy Combust. Sci.* **2010**, *36*, 260. [[CrossRef](#)]
14. Romano, M.C.; Spinelli, M.; Campanari, S.; Consonni, S.; Cinti, G.; Marchi, M.; Borgarello, E. The Calcium Looping Process for Low CO₂ Emission Cement and Power. *Energy Procedia* **2013**, *37*, 7091. [[CrossRef](#)]
15. Rodriguez, N.; Murillo, R.; Abanades, C. CO₂ Capture from Cement Plants Using Oxy-fired Pre-calcination and/or Calcium Looping. *Environ. Sci. Technol.* **2012**, *46*, 2460. [[CrossRef](#)] [[PubMed](#)]
16. Chen, J.; Duan, L.; Sun, Z. Review on the Development of Sorbents for Calcium Looping. *Energy Fuels* **2020**, *34*, 7806–7836. [[CrossRef](#)]
17. Tesio, U.; Guelpa, E.; Verda, V. Comparison of S_{CO2} and He Brayton Cycles Integration in a Calcium-Looping for Concentrated Solar Power. *Energy* **2022**, *247*, 123467. [[CrossRef](#)]
18. Teixeira, P.; Afonso, E.; Pinheiro, C.I.C. Tailoring Waste-Derived Materials for Calcium-Looping Application in Thermochemical Energy Storage Systems. *J. CO₂ Util.* **2022**, *65*, 102180. [[CrossRef](#)]
19. Sun, X.; Fang, D.; Zhang, L.; Duan, F.; Sun, Y. Performance Study of Modified Calcium Magnesium Acetate (MCMA) in the Process of High Temperature CO₂ Capture and the Application of Spent MCMA for Sequential SO₂ Removal. *Asia-Pac. J. Chem. Eng.* **2017**, *12*, 595–604. [[CrossRef](#)]
20. Teixeira, P.; Fernandes, A.; Ribeiro, F.; Pinheiro, C.I.C. Blending Wastes of Marble Powder and Dolomite Sorbents for Calcium-Looping CO₂ Capture under Realistic Industrial Calcination Conditions. *Materials* **2021**, *14*, 164379. [[CrossRef](#)] [[PubMed](#)]
21. Fahim, T.K.; Zaidul, I.S.M.; Abu Bakar, M.R.; Salim, U.M.; Awang, M.B.; Sahena, F.; Jalal, K.C.A.; Sharif, K.M.; Sohrab, M.H. Particle Formation and Micronization Using Non-Conventional Techniques—Review. *Chem. Eng. Process. Process Intensif.* **2014**, *86*, 47–52. [[CrossRef](#)]
22. Franco, P.; Sacco, O.; de Marco, I.; Sannino, D.; Vaiano, V. Photocatalytic Degradation of Eriochrome Black-T Azo Dye Using Eu-Doped ZnO Prepared by Supercritical Antisolvent Precipitation Route: A Preliminary Investigation. *Top. Catal.* **2020**, *63*, 1193–1205. [[CrossRef](#)]
23. Smith, P.J.; Kondrat, S.A.; Carter, J.H.; Chater, P.A.; Bartley, J.K.; Taylor, S.H.; Spencer, M.S.; Hutchings, G.J. Supercritical Antisolvent Precipitation of Amorphous Copper–Zinc Georgeite and Acetate Precursors for the Preparation of Ambient-Pressure Water-Gas-Shift Copper/Zinc Oxide Catalysts. *ChemCatChem* **2017**, *9*, 1621–1631. [[CrossRef](#)]
24. Miedziak, P.J.; Tang, Z.; Davies, T.E.; Enache, D.I.; Bartley, J.K.; Carley, A.F.; Herzing, A.A.; Kiely, C.J.; Taylor, S.H.; Hutchings, G.J. Ceria Prepared Using Supercritical Antisolvent Precipitation: A Green Support for Gold-Palladium Nanoparticles for the Selective Catalytic Oxidation of Alcohols. *J. Mater. Chem.* **2009**, *19*, 8619–8627. [[CrossRef](#)]
25. Reverchon, E.; della Porta, G.; di Trolio, A.; Pace, S. Supercritical Antisolvent Precipitation of Nanoparticles of Superconductor Precursors. *Ind. Amp Eng. Chem. Res.* **1998**, *37*, 952–958. [[CrossRef](#)]
26. Reverchon, E.; de Marco, I.; della Porta, G. Tailoring of Nano- and Micro-Particles of Some Superconductor Precursors by Supercritical Antisolvent Precipitation. *J. Supercrit. Fluids* **2002**, *23*, 81–87. [[CrossRef](#)]
27. Nobre, L.C.S.; Santos, S.; Palavra, A.M.F.; Calvete, M.J.F.; de Castro, C.A.N.; Nobre, B.P. Supercritical Antisolvent Precipitation of Calcium Acetate from Eggshells. *J. Supercrit. Fluids* **2020**, *163*, 104862. [[CrossRef](#)]
28. Cardoso, M.A.T.; Monteiro, G.A.; Cardoso, J.P.; Prazeres, T.J.V.; Figueiredo, J.M.F.; Martinho, J.M.G.; Cabral, J.M.S.; Palavra, A.M.F. Supercritical Antisolvent Micronization of Minocycline Hydrochloride. *J. Supercrit. Fluids* **2008**, *44*, 238–244. [[CrossRef](#)]
29. Teixeira, P.; Bacariza, C.; Mohamed, I.; Pinheiro, C.I.C. Improved Performance of Modified CaO-Al₂O₃based Pellets for CO₂ capture under Realistic Ca-Looping Conditions. *J. CO₂ Util.* **2022**, *61*, 102007. [[CrossRef](#)]
30. Stanmore, B.R.; Gilot, P. Review-Calcination and Carbonation of Limestone during Thermal Cycling for CO₂ Sequestration. *Fuel Process. Technol.* **2005**, *86*, 1707–1743. [[CrossRef](#)]

31. Silcox, G.D.; Kramlich, J.C.; Pershing, D.W. A Mathematical Model for the Flash Calcination of Dispersed CaCO_3 and $\text{Ca}(\text{OH})_2$ Particles. *Ind. Eng. Chem. Res.* **1989**, *28*, 155–160. [[CrossRef](#)]
32. Ruhaimi, A.; Aziz, M.; Jalil, A. Magnesium oxide-based adsorbents for carbon dioxide capture: Current progress and future opportunities. *J. CO₂ Util.* **2021**, *43*, 101357. [[CrossRef](#)]
33. Valverde, J.M.; Sanchez-Jimenez, P.E.; Perez-Maqueda, L.A. Ca-Looping for Post-combustion CO_2 Capture: A Comparative Analysis on the Performances of Dolomite and Limestone. *Appl. Energy* **2015**, *138*, 202–215. [[CrossRef](#)]

Disclaimer/Publisher’s Note: The statements, opinions and data contained in all publications are solely those of the individual author(s) and contributor(s) and not of MDPI and/or the editor(s). MDPI and/or the editor(s) disclaim responsibility for any injury to people or property resulting from any ideas, methods, instructions or products referred to in the content.